INVESTIGATION OF THE THERMAL BOUNDARY LAYER DEVELOPMENT LENGTH IN ANNULAR UPWARD HEATED SUPERCRITICAL FLUID FLOWS

JURRIAAN W. R. PEETERS
Delft University of Technology, Department of Radiation, Radionuclides and Reactors, section of Physics of Nuclear Reactors
Mekelweg 15, 2629 JB Delft, the Netherlands
jwrpeeters@gmail.com

CHRISTOPHE T'JOEN
Delft University of Technology, Department of Radiation, Radionuclides and Reactors, section of Physics of Nuclear Reactors

MARTIN ROHDE
Delft University of Technology, Department of Radiation, Radionuclides and Reactors, section of Physics of Nuclear Reactors

Abstract
Despite the harsh conditions they impose, supercritical fluids are being used more commonly today in industry. Supercritical water is being considered as a coolant in supercritical water reactor designs.
Heat transfer to supercritical fluids shows unusual behaviour, due to the sharp property variations with temperature. As a result the thermal boundary layer development length is expected to show unusual behaviour as well.
*In this paper the thermal boundary layer development length in supercritical CO_2 and water flowing through an annulus at laminar flow conditions is investigated numerically. An annulus configuration was selected as it is a typical geometry found in heat exchangers and nuclear reactors. The laminar flow condition has been chosen in order to fully focus on the effect that temperature variations have on the development of the thermal boundary layer and to exclude any influence turbulence models might induce.*
Relationships to predict the thermal boundary layer development length as a function of dimensionless ratio of wall heat flux and mass flux are proposed for water (25 MPa) and CO_2 (9.52 MPa). These relationships are based on numerical results as well as an analytical model. A recommendation is made to include inlet temperature effects.

INTRODUCTION
Supercritical fluids are fluids at a pressure above the critical pressure and at temperatures higher than the critical temperature. Such fluids experience sharp property variations with increasing temperature (especially near the pseudo-critical temperature T_{pc}, see figure 1) and do not undergo a phase change. Supercritical fluids are used today in power cycles and chemical extraction processes, but they are also being considered for refrigeration (see e.g. Lorentzen & Pettersen (1993)). Another possible application is the 'supercritical water reactor'. In this nuclear reactor, the fuel rods will be cooled by upward flowing supercritical water (25 MPa). It is important to accurately know the heat transfer phenomena during the design phase in order to prevent fuel cladding failure due to high temperatures.

Because the properties of supercritical fluids vary sharply with temperature, heat transfer to such fluids is not easily captured by well established heat transfer relationships (Pioro & Duffey (2005), Pioro et al. (2004), Duffey and Pioro (2004)).
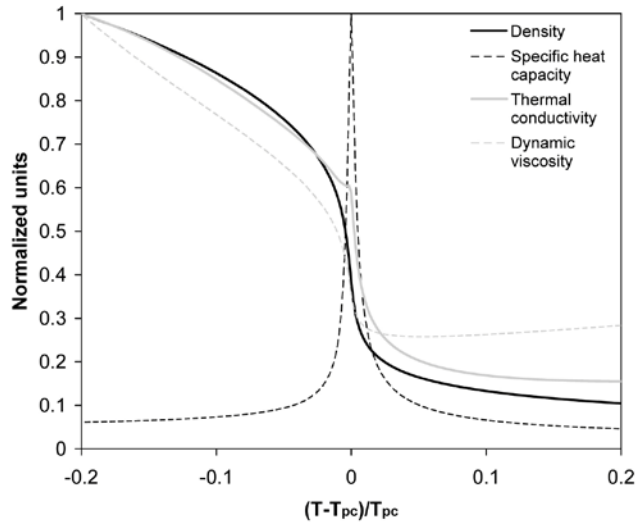
Figure 1: Normalized fluid properties as a function of non-dimensional temperature for supercritical water (25 MPa). Shown are $\rho/\rho(T=235\ ^oC)$, $\lambda/\lambda(T=235\ ^oC)$, $\mu/\mu(T=235\ ^oC)$ and $c_p/c_p(T_{pc}=385\ ^oC)$.

Many heat transfer experiments with turbulent supercritical fluid flows, reported a local peak in the heat transfer coefficient when the fluid temperatures are near the pseudo-critical temperature (the temperature for which the specific heat capacity has a maximum). Swenson et al. (1965) reported that this peak occurs when the 'film temperature' is near T_{pc}. Yamagata et al. (1972) found a peak in the heat transfer coefficient when the bulk temperature was near T_{pc}. Recent experimental investigations (Kim et al. (2007), Licht et al. (2008)) of heat transfer to supercritical fluids in annuli also show that the maximum in heat transfer coefficient occurs when the bulk enthalpy is slightly lower than the pseudo-critical enthalpy. The wall temperature then exceeds T_{pc}, so the sharp property change occurs in the boundary layer.

A parameter that is often used in the design of heat transfer equipment is the thermal development length. This parameter marks the region with the highest average heat transfer coefficient for sub-critical fluids. Little has been published regarding this parameter for supercritical fluids. The goal of this paper is therefore to study the thermal development length in supercritical fluids. To fully focus on the variable property effects on heat transfer and to exclude any effects turbulence might have, laminar flow conditions are chosen. Because the density varies sharply with temperature, buoyancy forces are important in upward heated supercritical fluid flows. This results in a combination of forced and natural convection, mixed convection. Laminar mixed convection of sub-critical fluids in various geometries has previously been investigated by various authors.

Hanratty et al. (1958) found analytically that buoyancy forces lead to M-shaped velocity profiles in a pipe. The fluid near the heated wall is accelerated, whereas the fluid in the middle of the pipe is decelerated. This effect can become so extreme, that the velocity becomes negative in the middle, which is called flow reversal. Hanratty et al. (1958) and Bernier and Baliga (1992) experimentally visualized the flow reversal phenomenon due to buoyancy forces in a pipe with a heated wall. Hanratty et al. (1958) report an increased heat transfer when an M-shaped velocity profile occurs. Wang et al. (1992) found that for stronger buoyancy forces (compared to inertia forces), heat transfer is locally enhanced for a pipe with a constant wall temperature T_w, especially if flow reversal occurs. Similar results were found by Desrayaud and Lauriat (2009) for a channel flow. Nesreddine et al. (1997) investigated upward mixed convection with a constant wall heat flux. They found that heat transfer is

enhanced for higher wall heat fluxes (which induce a strong buoyancy and velocity profile distortion).

Laminar supercritical water flowing upwards in a pipe with a uniform wall heat flux was numerically investigated by Jiang et al. 1995. They reported enhanced heat transfer. In a subsequent study, Jiang et al. (2008) (1) and Jiang et al. (2008) (2) numerically and experimentally investigated heat transfer to supercritical CO_2 at low Reynolds numbers. They found a local increase in heat transfer, which they attribute to a transition from laminar to turbulent flows.

Outline
This article is divided in to two parts. It starts with an analytical derivation to gain a qualitative insight into the variable properties effect on heat transfer. Subsequently, CFD-methods that were used are discussed, after which the CFD-results are presented. These are discussed at the end in combination with the analytical findings.

INTEGRAL APPROXIMATION METHOD
To gain a qualitative insight into the effect of variable properties on heat transfer, the integral approximation method is used to solve the transport equation for temperature:

$$\frac{\partial}{\partial x}\rho U c_p T = \frac{\partial}{\partial y}\lambda\frac{\partial T}{\partial y} \tag{1}$$

In this equation is ρ the density, c_p the specific heat capacity, U the axial velocity, λ the thermal conductivity and T the temperature. This equation holds only for *Pe>>1 (Deen 1998)* The problem under consideration is graphically represented in figure 2:
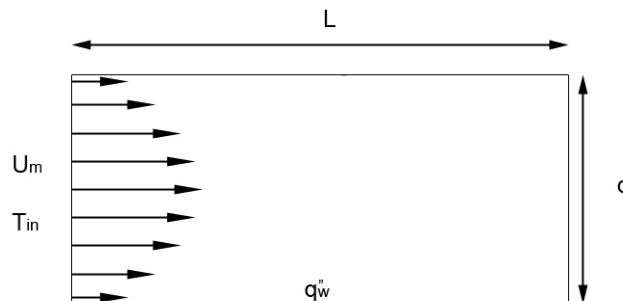
Figure 2: Graphic representation of the case considered. Fluid enters with a fully developed velocity profile and a uniform temperature T_{in}. One wall is adiabatic, and at the other wall a uniform heat flux is imposed.

Fluid enters a channel fully developed with an average flow velocity U_m:

$$U(y) = 6U_m\left(\frac{y}{d}-\frac{y^2}{d^2}\right) \tag{2}$$

The upper wall is considered to be adiabatic. At the lower wall, there is a uniform wall heat flux q''_w (W/m²K). The channel width is d (m), and the fluid enters with a temperature of T_{in} (K).
The first step of the integral approximation method is to assume a function to describe the temperature as a function of y over the thermal boundary layer thickness $\delta(x)$ (the length measured from the wall to the point in the fluid where $T=T_{in}$):

$$T - T_{in} = A + B\left(\frac{y}{\delta(x)}\right) + C\left(\frac{y}{\delta(x)}\right)^2 + D\left(\frac{y}{\delta(x)}\right)^3 + E\left(\frac{y}{\delta(x)}\right)^4 \qquad (3)$$

The constants A, B, C, D and E are evaluated with the boundary conditions in the system: $T_y(0) = -q''_w/\lambda_w$, $T(\delta(x))=T_{in}$, $T_y(\delta(x))=0$, $T_{yy}(\delta(x))=0$, $T_{yy}(0)=0$ (the subscripts indicate derivatives). This results in the following temperature profile:

$$T(x, y) = \frac{q''_w}{\lambda_w}\left(\frac{\delta(x)}{2} - y + \frac{y^3}{\delta^2(x)} - \frac{y^4}{2\delta^3(x)}\right) + T_{in} \qquad (4)$$

In which λ_w (W/mK) is the thermal conductivity of the fluid at the wall. To make equation 4 less cumbersome, the Lévêque approximation is used for the velocity, which is a first order Taylor approximation around $y=0$. For constant properties, $\lambda_w=\lambda$.

Substituting equation **(4)** in equation **(1)** and integrating the result from 0 to $\delta(x)$ yields a differential equation for $\delta(x)$:

$$\frac{3}{5}\rho U_m c_p \delta^2(x)\left(\frac{d\delta(x)}{dx}\right) - \lambda d = 0 \qquad (5)$$

Which has the solution

$$\frac{\delta(x)}{d} = \frac{1}{2}40^{1/3} Pe^{-1/3}\left(\frac{x}{d}\right)^{1/3} \qquad (6)$$

This equation forms, together with equation **(4)**, the solution of the temperature field in the developing region. Equation **(6)** is valid for a fluid with constant properties.

Variable properties
Three different cases are considered here: variable density, specific heat capacity and thermal conductivity. The variation of the properties is modeled as a linear function of temperature:

$$\psi(T) - \psi(T_{in}) = \psi_{in}\zeta_\psi(T(x, y) - T_{in}) \qquad (7)$$

In which ψ is ρ, c_p or λ and in which ζ_ψ (1/K) is:

$$\zeta_\psi = \frac{1}{\psi_{in}(T_{in})}\left(\frac{d\psi}{dT}\right)_{T_{in}} \qquad (8)$$

For $\psi = \rho$, $\zeta_\rho = \beta$, which is known as the thermal expansion coefficient. Using these property relations together with equations **(1)** and **(4)** and repeating the same steps as before, a relationship is derived for the thermal boundary layer thickness. For $\rho(T)$ and $c_p(T)$, the solution for the boundary layer thickness $\delta(x)$ is:

$$\frac{17}{84}\zeta_\psi\frac{q''_w}{\lambda}Pe\,\delta^4(x) + (1+\zeta_\psi T_{in})Pe\,\delta^3(x) - \frac{630}{126}xd^2 = 0 \qquad (9)$$

Equation **(9)** forms the solution of the temperature field for cases with variable density or specific heat capacity. It was assumed here that the density changes are small and do not influence the velocity field (neglecting acceleration).

To model thermal conductivity as a function of temperature, λ_w in equation **(4)** needs to be evaluated. Using equation **(7)** together with **(4)** and evaluating the result for $y=0$ yields for λ_w:

$$\lambda_w = \frac{1}{2}\lambda_{in} \pm \frac{1}{2}(\lambda_{in}^2 + \lambda_{in}\zeta_\lambda q_w''\delta(x))^{1/2} \tag{10}$$

The solution with the minus is dropped here: if q"$_w$ is zero, then λ_w should be λ_{in}. Using (10) together with (1), and (4) and taking the same steps as before yields a relationship for the boundary layer thickness for variable thermal conductivity:

$$\delta(x) = \frac{30^{1/3}}{\lambda_{in}Pe}\left(\left(\left(\int_0^x \frac{f(x')}{\lambda_{in}+10\lambda_{in}f(x')}dx'\right)\lambda_{in} + 2\left(\int_0^x \frac{f^2(x')}{\lambda_{in}+10\lambda_{in}f(x')}dx'\right)\right)\lambda_{in}^2 Pe^2\right)^{1/3} \tag{11}$$

In which f(x') = λ_w(x)-0.5λ_{in}. It was assumed here that f(x) is always real and that x ≥ 0. Equation (11), together with equation (4), form the solution of the temperature field for variable thermal conductivity.

Equations (9) and (11) show that the boundary layer thickness is a function of multiple dimensionless groups:

$$\frac{\delta(x)}{d} = f\left(Pe, \frac{\beta q_w''d}{\lambda_{in}}, \frac{\zeta_{cp}q_w''d}{\lambda_{in}}, \frac{\zeta_\lambda q_w''d}{\lambda_{in}}, \beta T_{in}, \zeta_{cp}T_{in}, \zeta_\lambda T_{in}\right) \tag{12}$$

The 2nd through 4th dimensionless groups represent the property changes in the system, whereas the last three represent the effect of the inlet temperature. The Peclet number is the ratio of the axial convective heat transfer rate to the axial conductive heat transfer rate.

Results
Because the relationships presented cannot be solved analytically, the thermal profiles *T(x,y)* and Nusselt numbers were calculated with Maple11 for four cases (flow with constant properties, variable density, variable specific heat capacity or variable thermal conductivity). The Nusselt number is defined as,

$$Nu = \frac{htc(x)\,d}{\lambda(T_{in})} \tag{13}$$

where the heat transfer coefficient *htc* is defined as:

$$htc(x) = \frac{q_w''}{T_w(x)-T_b} \qquad \text{with} \qquad T_b = \frac{\int_0^d \rho U c_p T dy}{\int_0^d \rho U c_p dy} \tag{14}$$

Where T_w is the wall temperature, T_b the bulk temperature and *q"$_w$* the wall heat flux.
The inlet properties and the uniform wall heat flux (*y=0*) are given in table 1. The average inlet flow velocity is 0.05 m/s.

Table 1: Selected conditions for the analytical case. The values listed correspond to supercritical CO_2 at 9.52 MPa.

T_{in} (°C)	ρ_{in} (kg/m^3)	$c_{p,in}$ (J/kgK)	λ (W/mK)	ζ_ρ (1/K)	ζ_{cp} (1/K)	ζ_λ (1/K)	q"$_w$ (W/m^2)
25.18	808	0.0898	2990	-0.0114	0.0270	-0.0146	5000

It was assumed here that the density and thermal conductivity decreases with temperature, whereas the specific heat capacity increases. This corresponds qualitatively with a supercritical fluid where $T_{in} < T_{pc}$.

The temperature profiles at x/d=25 are plotted as a function of the coordinate y/d for the four cases in Figure 3(left). It can be seen that a decreasing density leads to higher temperatures at the wall (lowering Nu) and that an increasing specific heat capacity leads to lower temperatures at the wall compared to the constant property case. The result for variable density ignores acceleration, which is not likely to be accurate for supercritical fluids. It is known from literature that a fluid accelerated by buoyancy forces in upward laminar flows causes a local increase in heat transfer. It can be seen in Figure 3(left) that decreasing thermal conductivity, leads to a higher temperatures near the wall and to lower temperatures far away from the wall. This leads in turn to a lower Nusselt number, as can be seen in Figure 3 (right).
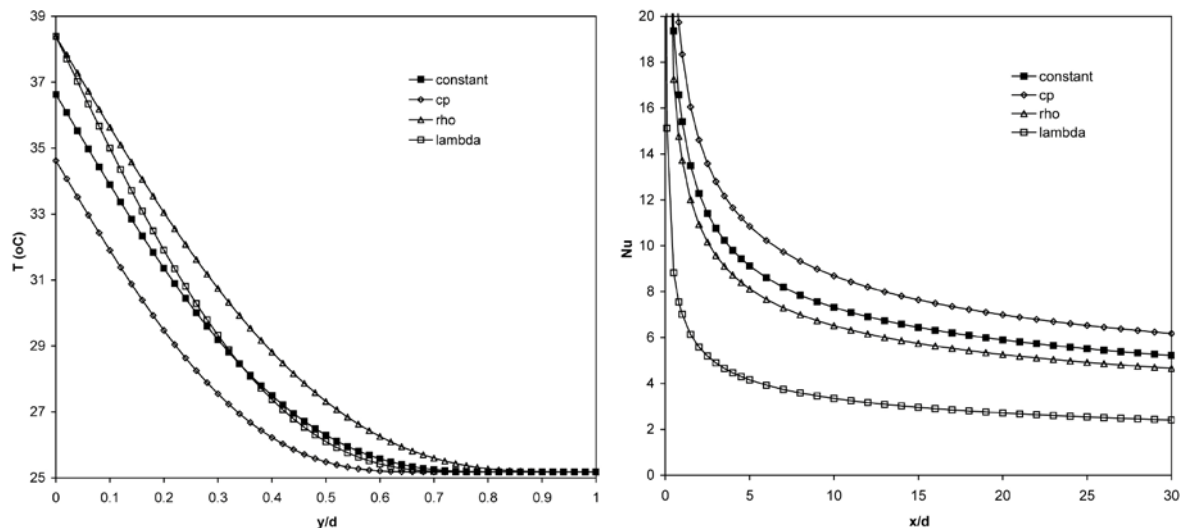
Figure 3: Left: temperature profiles (x/d=25) for four different cases: constant properties, variable c_p, ρ, λ. **Right:** Nusselt numbers as a function of the axial length.

From the analytical derivations and results above, it can be seen that the thermal boundary layer thickness is increased for decreasing density (not considering acceleration effects) and decreased for increasing specific heat capacity. These changing properties lead to lower and higher Nusselt numbers, respectively. Decreasing thermal conductivity causes the thermal boundary layer and the Nusselt number to become smaller.

CFD-METHODS

Numerical model
To model heat transfer to supercritical fluids, the open source C++ toolbox OpenFOAM 1.7.1 was used.

Equations
In the code three variables are solved for: the velocity U, the enthalpy h and the total pressure p. The steady-state Navier-Stokes equations governing laminar supercritical fluid flows can be written as follows (Todreas and Kazimi 1990):

the momentum equation,

$$\nabla \cdot \rho \overline{U}\overline{U} = \nabla \cdot \overline{\overline{\tau}} - \nabla p + \rho \overline{g} \tag{15}$$

where τ is defined as:

$$\overline{\overline{\tau}} = \mu \left(\left(\nabla \overline{U} \right) + \left(\nabla \overline{U} \right)^T - \frac{2}{3} \left(\nabla \cdot \overline{U} \right) I \right) \tag{16}$$

and the enthalpy equation:

$$\nabla \cdot \rho \vec{U} h = \nabla \cdot \frac{\lambda}{c_p} \nabla h \tag{17}$$

The work and dissipation terms are neglected in the enthalpy equation, because their order of magnitude is much smaller than the convective and diffusive terms (this was verified with preliminary simulations). The continuity equation reads:

$$\nabla \cdot \rho \vec{U} = 0 \tag{18}$$

This equation is satisfied through the SIMPLE-algorithm.

Boundary conditions
For all walls the no-slip boundary condition is used for velocity. For the inlet a fully developed velocity profile (2) and a uniform enthalpy profile are considered, whereas for the outlet a zero gradient condition is used for the velocity. For the outlet enthalpy boundary condition, the enthalpy gradient value of the before last cell with respect to the axial direction is used as a boundary condition at the outlet. For a wall with a uniform heat flux, the following boundary condition is used:

$$\vec{n} \cdot \nabla h = \left(\frac{c_p}{\lambda} \right)_f q_w'' \tag{19}$$

in which the subscript f denotes the wall face values of c_p and λ.

Fluid properties
As was mentioned before, supercritical fluid properties change sharply as the enthalpy increases, especially near the pseudo-critical point. This behaviour is modeled with splines:

$$\psi_i(h) = \psi_{a,i}(h - h_i)^3 + \psi_{b,i}(h - h_i)^2 + \psi_{c,i}(h - h_i) + \psi_{d,i} \quad \text{for} \quad h_i \leq h < h_{i+1} \tag{20}$$

In which ψ_i is a fluid property (ρ, c_p, λ, μ) or T. $\psi_{(abcd),i}$ are constants unique for each property and particular enthalpy range. The splines were made with no less than 40 data points from the NIST-database over a temperature range of 10-150 ^{o}C for CO_2 at 9.52 MPa and 1-1000 ^{o}C for water at 25 MPa. The spline- interpolated values were compared with the NIST-database. It was found that the spline-values predict the NIST-database values very well. The spline interpolated values deviated less than 0.1% from the NIST-database on average.

Discretization, relaxation and convergence criteria
Each term in the Navier-Stokes equations (as written above) is discretized using a central differencing scheme, except for the convective terms, which are discretized using a 1st order upwind differencing scheme. To ensure numerical stability, relaxation factors are used. An optimum between total calculation time and convergence was found when setting the relaxation factors for U, h, p to 0.4, 0.5 and 0.3, respectively. The following criteria for convergence are used: the average of $\nabla \cdot \rho \vec{U}$ is of order 10^{-6} and the change in temperature values at the outlet < 0.01 K for 1000 iterations.

Validation

To ensure that the code works properly, it was validated against results reported by Jiang et al. 2008 (1). They reported both CFD and experimental results for supercritical CO_2 (9.52 MPa) flowing upwards in a vertical pipe with a uniform wall heat flux q''_w. Results from the OpenFOAM code were compared with CFD and experimental results from Jiang et al. 2008 (1). In Figure 4 (left) the velocity profiles for different axial positions as calculated by the OpenFOAM code are compared with the CFD results from Jiang et al. 2008 (1). It can be seen that there is excellent agreement between them. On the right, heat transfer coefficient results from the OpenFOAM code are compared with experimental values from Jiang et al. 2008 (1). There is good agreement for x/d<15. After x/d>15 the OpenFOAM results do not match well. Jiang et al. state that this is due to a transition from laminar to turbulent flow. The code used in the present study is not able to capture turbulent effects, because of the steady state formulation of the equations and the lack of turbulence modeling. A large number of extra validation cases was considered, and these all indicated that the code is able to properly simulate the heating of supercritical fluids.
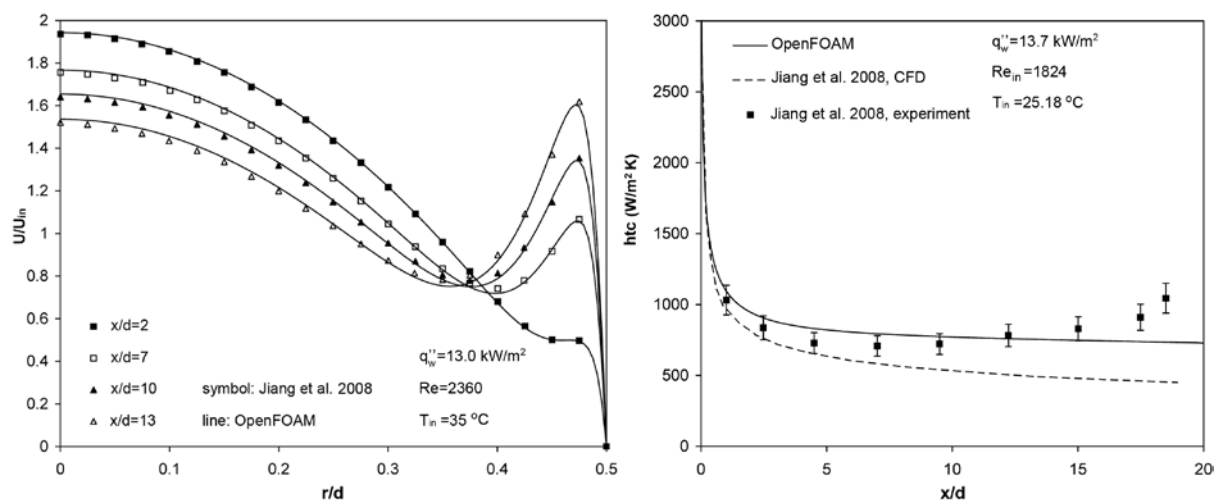

Figure 4: Left: Velocity profiles as a function of the pipe radius at different axial positions. **Right:** Heat transfer coefficient along the axial length.

Results

Heat transfer to supercritical CO_2 (9.52 MPa) and supercritical water at 25 MPa were simulated for different system parameters (inlet mass flux, wall heat flux) in an annular geometry (see Figure 5). The hydraulic diameter is $d=2(R_o-R_i)$ = 1 mm. Supercritical fluid enters the annulus fully developed with a uniform enthalpy (temperature) profile. The length of the annulus is $L=200d$. The outer wall is considered to be adiabatic and at the inner wall there is a uniform wall heat flux q''_w. The mesh is a wedge geometry with the number of cells set to 2000 × 100 cells (axial × radial). Supercritical CO_2 (9.52 MPa) was mainly investigated. Average inlet velocities were varied from 0.03 to 0.07 m/s (Pe=807-1883) and the wall heat flux was varied from 2 to 10 kW/m^2. The inlet temperature is T_{in}=25.18 ^{o}C which is much lower than the pseudo-critical temperature T_{pc}=42.66 ^{o}C. The highest Reynolds number simulated was 785, to ensure that the flow was laminar.
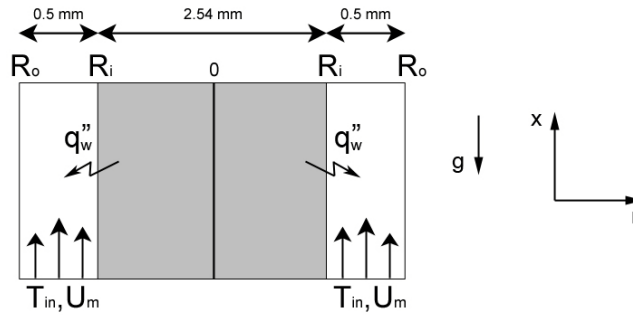
Figure 5: Graphic representation of the investigated case.

Heat transfer phenomena

In figure 5, the heat transfer coefficients along the length of the annulus for five different wall heat fluxes are shown. It can be seen that increasing the wall heat flux causes an increase in the heat transfer coefficient, up to a certain position x/d. Two cases show a maximum in heat transfer coefficient. This maximum is located between the position x/d where the wall temperature equals the pseudo-critical temperature and the position where the bulk temperature equals the pseudo-critical temperature. It was found for all cases that the fluid near the wall is accelerated over the entire length of the annulus, which causes an increase in the heat transfer coefficient.
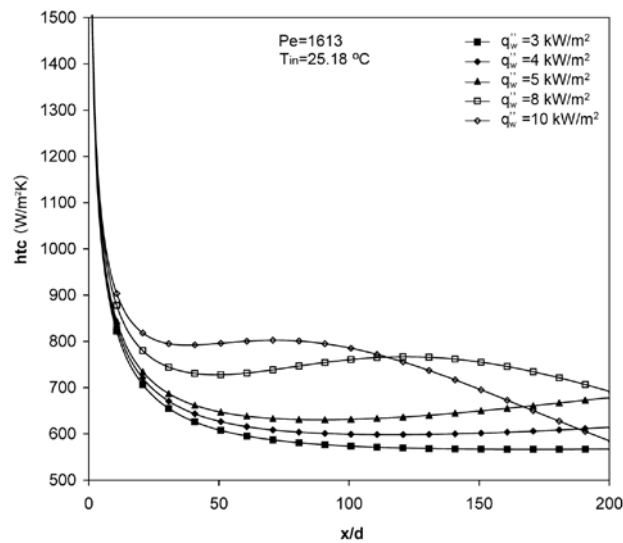
Figure 6: Heat transfer coefficients for different wall heat fluxes as a function of the length of the annulus.

From the analytical results presented above it is known that an increase in specific heat capacity causes an increase in heat transfer coefficient, whereas a decrease in thermal conductivity causes a decrease in the heat transfer coefficient. Therefore, an increase in the heat transfer coefficient (as seen in figure 6) is caused by an increase in specific heat capacity and acceleration, which outweigh the effect of the decreasing thermal conductivity. A decrease in the heat transfer coefficient is caused by a decrease in thermal conductivity and specific heat capacity, which then outweigh the acceleration effect on heat transfer.

Thermal boundary layer development length

Shah and London (1978) define the thermal development length as the length it takes for the Nusselt number to become (nearly) constant. A position where the heat transfer coefficient was constant was however not found within the investigated domain. Instead, to quantify the

behaviour of the thermal boundary layer development, the local minimum in heat transfer coefficient was investigated, because it can be regarded as the position where the inlet effect (sharp decrease of *htc* near the inlet) is no longer apparent and where heat transfer starts to be dominated by the property variations. The length measured from the inlet to the position of a local minimum is denoted here as L_{thb} and it is called here the *thermal boundary layer development length*. This position is interesting because it signifies the region with the highest average heat transfer coefficients starting from the inlet.

It was found that L_{thb} was the same for different cases if the ratio of the wall heat flux over the mass flux was the same. Heat transfer phenomena were investigated for four different mass fluxes and different wall heat fluxes. For all these cases, L_{thb} was recorded and these values were plotted against a non-dimensionless ratio of the wall heat flux and mass flux. The first two dimensionless groups of equation (12) were used. The result is shown in figure 7 (left). It can be seen that L_{thb} can be well represented by a power regression (also shown in the figure). The regression line predicts the numerical data within 6%. The results show that L_{thb} becomes smaller with increasing wall heat flux or decreasing mass flux. This can be explained as follows: with a higher heat flux or lower mass flux, the local temperature increase faster. The specific heat capacity increases faster as well, causing the position of the local minimum in *htc* to shift towards the inlet.
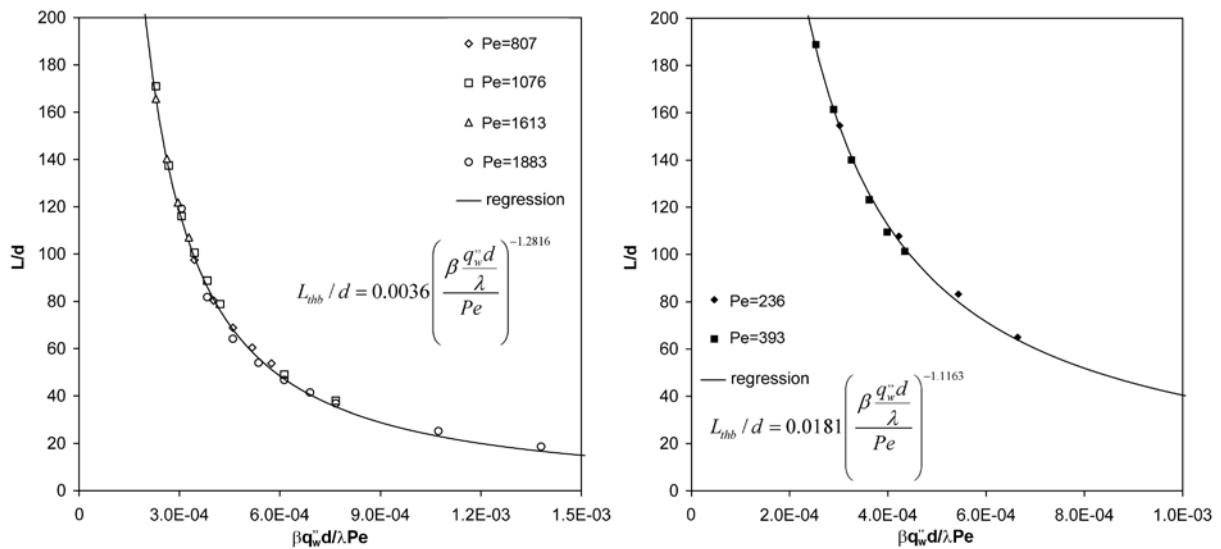
Figure 7: left: L_{thb} plotted against a non-dimensionless ratio of the wall heat flux and mass flux for CO_2 (9.52 MPa) cases. **Right**: the same, but for supercritical water (25 MPa). β was evaluated at T_{in}.

The exact same system as described above was investigated for supercritical water (25 MPa) as well, but with an inlet temperature of 330 ^oC. Similar results as those for supercritical CO_2 were obtained, as shown in figure 7 (right). The results of L_{thb} in this case are predicted within 5% by the regression line. The difference in the power regressions can be explained by the different property variation of supercritical CO_2 and water. The properties of supercritical water (25MPa) vary more sharply than for supercritical CO_2 (9.52 MPa).

DISCUSSION

With a semi-analytical model, it has been shown that varying fluid properties affect the heat transfer: an increasing specific heat capacity enhances heat transfer. A decreasing thermal conductivity lowers the heat transfer. These qualitative results were combined with results from literature to explain the numerical results of supercritical CO_2 flowing upwards through an annulus, heated by a uniform wall heat flux. The heat transfer coefficients show a local

increase due to the increase of c_p and due to flow acceleration. For higher heat fluxes and lower inlet mass fluxes, the local increase shifts towards the inlet. If the heat flux is high enough, or if the inlet mass flux is low enough, the heat transfer first increases and then decreases, because c_p decreases again, even though the flow keeps accelerating.

Relationships to predict the position of the local minimum in heat transfer coefficient were proposed for supercritical CO_2 and water. It was found that these relationships do not work well for different inlet temperatures. To include the effect of the inlet temperature in the relationships, the change of the properties in the system should be included. To do this, the dimensionless groups from equation (12) that were not yet considered could be used. The parameters β, ζ_{cp} and ζ_λ could be averaged between the inlet temperature and a reference temperature (for example T_{pc}).

The relevance of the newly proposed length L_{thb} can be explained as follows: this length signifies the region with the largest *htc*. The position $x=L_{thb}$ is the position where the inlet effect is no longer apparent and where the variation of the properties start to become dominant. If the effect of the inlet temperature can be included in the relationships for L_{thb}, such relationships would be very useful in the design of laminar heat transfer equipment (such as for refrigeration) and for experimental facilities. Possibly, similar relations can be found for the position where the heat transfer coefficient has a subsequent maximum.

Because the results presented here are based on CFD results, it is important to check if the results are independent of the mesh size. To this end, a mesh sensitivity analysis was performed for the case with the highest wall heat flux, which was presented in figure 6. Two mesh-sizes were used (2000×100 and 1500×100). The position of the local minimum of the second mesh deviated less than 0.1% with respect to the position obtained with the larger mesh. This result adds to the credibility of the relationships.

REFERENCES

Bernier, M. A. and Baliga, B. R., 1992, "Visualization of upward mixed-convection flows in vertical tubes with uniform wall heat flux", International Journal of Heat and Fluid Flow, vol. 13, pp. 241-249.

Deen, W. M. 1998, "Analysis of transport phenomena", Oxford University Press.

Desrayaud, G. and Lauriat, G., 2009, "Flow reversal of laminar mixed convection in the entry region of symmetrically heated, vertical plate channels", International Journal of Thermal Sciences, vol. 48, 2036-2045.

Duffey, R.B., Pioro, I.L., 2004, "Experimental heat transfer of supercritical carbon dioxide flowing inside channels", Nuclear Engineering and Design, vol. 235, pp.913-924.

Fischer, K., Schulenberg, T. & Laurien, E., 2009, "Design of a supercritical water-cooled reactor with a three pass core arrangement", Nuclear Engineering and Design, vol. 239, pp. 800-812.

Hanratty, T. J., Rosen, E. M. and Kabel, R. L., 1958 "Effect of heat transfer on flow field at low Reynolds numbers in vertical tubes", Industrial and Engineering Chemistry, vol. 50, pp. 815-820.

Jiang, P.X., Ren, Z. P. and Wang, B. X., 1995, "Convective heat and mass transfer in water at super-critical pressures under heating or cooling conditions in vertical tubes, Journal of Thermal Sciences, vol. 4, pp.15-25.

Jiang, P.X., Zhang, Y., xu, X. J. and Shi, R. F. 2008 (1), "Experimental and numerical investigation of convective heat transfer of CO_2 at supercritical pressures in a vertical tube at low Reynolds numbers", International Journal of Thermal Sciences, vol. 47, 998-1011.

Jiang, P.X., Zhang, Y., Zhao, C. R. and Shi, R. F., 2008 (2), "Convection heat transfer of CO_2 at supercritical pressures in a vertical mini tube at relatively low Reynolds numbers", Experimental Thermal and Fluid Science, vol. 32, pp. 1628-1637.

Kim, H. Y., Kim, H., Kang, D. J., Song, J. H. and Bae, Y. Y., 2007, "Experimental investigations on heat transfer to CO_2 flowing upward in a narrow annulus at supercritical pressures", Nuclear Engineering and Technology, vol. 40, pp. 155-162.

Licht, J., Anderson, M. and Corradini, M. 2008, Heat transfer to water at supercritical pressures in a circular and square annular flow geometry", International Journal of Heat and Fluid Flow, vol. 29, pp. 155-166.

Lorentzen, G. & Pettersen, J., 1993, "A new efficient and environmentally benign system for car air-conditioning", International Journal of Refrigeration, vol. 21 (3), pp. 180-193.

Nesreddine, H., Galanis, N. and Nguyen, C. T., 1997, "Variable-property effects in laminar aiding and opposing mixed convection of air in vertical tubes", Numerical Heat Transfer, Part A: Applications, vol. 31, pp. 53-69.

NIST REFPROP, 2007, "reference fluid thermodynamic and transport properties, database 23, version 7.

Pioro, I.L. & Duffey, R.B., 2005, "Experimental Heat Transfer in Supercritical Water Flowing Inside Channels", Nuclear Engineering and Design vol. 235, pp. 2407-2430.

Pioro, I.L., Khartabil, K. H. & Duffey, R.B., 2004, "Heat transfer to supercritical fluids flowing in channels – empirical correlations (survey)", Nuclear Engineering and Design, vol. 230, pp. 69-91.

Shah, R.K. and London, A.L., 1978, "Laminar flow forced convection in ducts", Academic Press.

Swenson, H. S., Carver, J.R. and Karakala, C. R., 1965, "Heat transfer to supercritical water in smooth-bore tubes", Journal of Heat Transfer, ASME Ser. C 87 (4), pp. 477-484.

Todreas, N.E. and Kazimi, M.S., 1990, "Nuclear systems I: Thermalhydraulic fundamentals", Taylor and Francis Group, TCC.

Wang, M., Tsuji, T., Nagano, Y., 1992, "Mixed convection with flow reversal in the thermal entrance region of horizontal and vertical pipes., International Journal of Heat and Mass Transfer, vol. 37, pp. 2305-2319.

Yamagata, K., Nishikawa, K., Hasegawa, S., Fujii, T., Yoshida, S., 1972, "Forced convective heat transfer to supercritical water flowing in tubes", International Journal of Heat and Mass Transfer, vol.15, pp. 2575-2593.